



Synthesis and characterization of 5-alkoxycarbonyl-4-hydroxymethyl-5-alkyl-pyrroline N-oxide derivatives

Anjan Patel^a, Natascha Rohr-Udilova^b, Thomas Rosenau^a, Klaus Stolze^{c,*}

^a Department of Chemistry, University of Natural Resources and Life Sciences (BOKU), Muthgasse 18, A-1190 Vienna, Austria

^b Division of Gastroenterology and Hepatology, Department of Internal Medicine III, Medical University of Vienna, Währinger Gürtel 18-20, A-1090 Vienna, Austria

^c Institute of Pharmacology and Toxicology, Department of Biomedical Sciences, University of Veterinary Medicine Vienna, Veterinärplatz 1, A-1210 Vienna, Austria

ARTICLE INFO

Article history:

Received 20 May 2011

Revised 12 September 2011

Accepted 7 October 2011

Available online 18 October 2011

Keywords:

EPR

Spin trapping

Superoxide

EMPO derivatives

Mitochondria

ABSTRACT

The syntheses, analytical properties, and spin trapping behavior of four novel EMPO derivatives, namely 5-ethoxycarbonyl-4-hydroxymethyl-5-methyl-pyrroline N-oxide (EHMPO), 5-ethoxycarbonyl-5-ethyl-4-hydroxymethyl-pyrroline N-oxide (EEHPO), 4-hydroxymethyl-5-methyl-5-propoxycarbonyl-pyrroline N-oxide (HMPPPO), and 4-hydroxymethyl-5-methyl-5-iso-propoxycarbonyl-pyrroline N-oxide (HMiPPPO), towards different oxygen- and carbon-centered radicals are described.

© 2011 Elsevier Ltd. All rights reserved.

1. Introduction

In previous studies about DEPMPO and EMPO derivatives,^{1–7} the stability of superoxide adducts was a central issue. Recent developments in the area of mitochondria-targeted spin traps that carry a phosphonium moiety as the mediating group (e.g., mito-DEPMPO^{8–10}) gave us impetus to focus on the synthesis of structurally related spin traps. The basic idea was that of a building block system with functional groups to which such mitochondria-viable groups or other site-selective moieties could be readily attached. This way, the spin traps with and without the special mitochondria-targeting group can be easily compared, the synthesis of the special derivatives just requiring attachment of the site-selective group rather than de novo synthesis of the whole spin trap molecule. For this purpose, we selected spin traps derived of EMPO or DMPO¹¹ bearing a 4-hydroxymethyl side chain, to which phosphonium groups or other mitochondria-targeting functionalities can readily be attached. The 4-hydroxymethyl group was advantageous because of two reasons: the synthesis of the starting materials was not too complex, and the hydroxy group offered many options for further modification, mainly by mild esterification procedures.

Since our initial approach to synthesize the 4-hydroxymethyl derivatives of EMPO directly from 1,4-butanediol and ethyl 2-nitropropanoate was not successful, we continued our efforts with 5-

hydroxymethyl derivatives of DMPO carrying either the THP or THF protecting group. While the synthesis provided the compounds in good yields, the corresponding DMPO derivatives, HMMPO, FMMPO, and PMMPO,¹¹ unfortunately did not show significantly better spin trapping properties compared to DMPO itself. Synthesis of the THP-protected EMPO derivatives, followed by a deprotection step leading to the free 4-hydroxymethyl derivatives was the logical next step: in the present paper we would like to communicate structure and properties of the four novel EMPO derivatives, 5-ethoxycarbonyl-4-hydroxymethyl-5-methyl-pyrroline N-oxide (EHMPO), 5-ethoxycarbonyl-5-ethyl-4-hydroxymethyl-pyrroline N-oxide (EEHPO), 4-hydroxymethyl-5-methyl-5-propoxycarbonyl-pyrroline N-oxide (HMPPPO), and 4-hydroxymethyl-5-methyl-5-iso-propoxycarbonyl-pyrroline N-oxide (HMiPPPO). All compounds were comprehensively analytically characterized by IR (Table 1), ¹H, ¹³C (APT), and NOESY NMR. The spin trapping activity of these compounds towards different carbon-centered radicals derived from methanol, ethanol, and formic acid, generated in the presence of a Fenton-type system, is also reported.

2. Results

2.1. Synthesis and chemical structure

The spin traps presented in this study are structurally related to the compound 5-ethoxycarbonyl-5-methyl-1-pyrroline-N-oxide (EMPO)^{12,13}, to which an additional 4-hydroxymethyl substituent

* Corresponding author.

E-mail address: Klaus.Stolze@vetmeduni.ac.at (K. Stolze).

Table 1
IR data [cm⁻¹] of the spin traps EHMPPO, EEHPO, HMPPPO, and HMiPPPO

EMPO ^a	2985	2940	2874	1741	1582	1464	1446	1377	1341	1288	1236	1182	1107	950	862	796	—
DMPO ^b	3086	2974	2933	2872	1662	1583	1458	1367	1344	1271	1232	1144	1117	714	584	507	—
EHMPPO	3307	3091	2983	2927	2904	2877	2843	1741	1589	1446	1379	1369	1329	1053	1024	986	696
EEHPO	3327	3087	2980	2941	2902	2885	2843	1741	1585	1466	1446	1387	1265	1095	1061	1030	696
HMPPPO	3302	3091	2968	2927	2879	2843	1741	1587	1462	1379	1327	1281	1165	985	949	696	—
HMiPPPO	3307	3091	2983	2927	2877	2843	1738	1587	1456	1377	1338	1325	1282	1053	1034	986	833
																	696

Intensities: **strong** (1741), **medium** (1464), **weak** (950).

^a Data from Stolze et al. (2003)⁴

^b Data from Stolze et al. (2011)¹¹

has been introduced. In addition, the effect of modification of the two substituents in position 5 of the pyrroline ring was also studied. The structures of the targets are shown in Figure 1a, the respective synthetic steps are given in Figure 1b.

The THP-monoprotected 1,4-butene-diol (**5**) was obtained in good yields by reaction of (*Z*)-but-2-ene-1,4-diol with 3,4-dihydro-2*H*-pyran in methylene chloride and tetrahydrofuran in the presence of catalytic amounts of *p*-toluenesulfonic acid monohydrate.¹⁴ Oxidation of the remaining free OH group to the aldehyde stage was effected by pyridinium chlorochromate (PCC), affording (*E*)-4-(tetrahydro-2*H*-pyran-2-yl)oxybut-2-enal (**6**) with high efficiency.¹⁵ The subsequent Michael addition of the nitro derivative in the presence of a catalytic amount of triethylamine in CH₃CN afforded **7a–d** as diastereomeric mixture which was not separated at this stage. Reductive cyclization with Zn-dust/NH₄Cl in THF/H₂O provided the THP-protected N-oxides (**8a–d**). Care has to be taken as to the absence of light and oxygen (argon atmosphere) during the reaction to avoid discoloration of the mixture and side reactions.^{4,13,16–18} The removal of the THP protecting group was performed in high yields by the catalytic action of hydrochloric acid.¹¹

2.2. Superoxide radical adducts

Figure 2 shows the EPR spectra of the respective superoxide adducts. The general method used for the generation of superoxide radicals was incubation of the spin traps (20 mM) in the presence of 0.2 mM hypoxanthine and 150 mU/ml xanthine oxidase (Xa/XOD) in 20 mM oxygenated phosphate buffer pH 7.4, containing 1 mM DTPA. When the maximum ESR intensity was reached after 7 min, SOD (150 U/ml) and catalase (250 U/ml) was added to stop superoxide production. Decay kinetics of the superoxide adducts were calculated as follows: A series of repetitive scans was recorded for each incubation (every 90 s for 30 min) using a first-order exponential decay approximation (Table 2, Pearson correlation coefficient $R^2 > 0.98$). In order to correct for the degradation products (a combination of the hydroxyl radical adduct and additional, not identified products) the respective contributions were subtracted from the individual spectra. The spectral contribution of the secondary products (as difference spectra) was obtained by subtracting the spectra taken from 0 to 6 min from those obtained between 7.5 and 15 min. The resulting ESR spectra were obtained from EHMPPO (Fig. 2a), EEHPO (Fig. 2b), HMPPPO (Fig. 2c), and HMiPPPO (Fig. 2d).

Whereas EHMPPO and HMPPPO showed similar EPR spectra (three different superoxide adducts with concentration ratios of around 2:1:1 and half lives of around 9–10 min), a slightly different product ratio was found with HMiPPPO, all having half lives of around 11 min. The behavior of EEHPO, on the other hand, was completely different. The stability of the superoxide adduct was considerably higher (28.4 min) and the lines were very broad, thus making a differentiation between the different isomers impossible. In Figure 3 we demonstrate in detail, how the simulations were obtained. From the EPR spectrum of EHMPPO/OOH (Fig. 3a, also shown above in Fig. 2a) the simulation of the first species (Fig. 3b) was subtracted. From the remaining difference spectrum (Fig. 3c) the second simulated spectrum (shown in Fig. 3d) could be subtracted, leaving the third species as the remaining lines (Fig. 3e). Since additional species (marked with asterisks in Fig. 3a) were also present, the simulation does not give a perfect fit. In addition, the presence of 2 asymmetric carbon centers in the spin trap (2 in the H adduct, 3 in the other radical adducts) leads to the formation of 4 diastereomeric radical adducts (2 in the case of H adducts). Furthermore, additional rotamers might also be formed.¹⁹ Due to the limited resolution of the spectrum not all possible species can be resolved. In addition, the high number of contributing species makes an unequivocal

interpretation of the spectrum difficult. In this respect it is not clear whether the different linewidth observed between lines 1 and 2 (Fig. 3c) can be explained in terms of two species showing only small differences in HFS and g -values (with a small HFS of 1.48 G), or whether the value of 1.48 G represents the difference between the hydrogen HFS of two different diastereomeric isomers (Fig. 3d, simulation, and Fig. 3e, remaining lines after subtraction of '3d' from '3c'). In order to be consistent with the spin trap HMiPPO, we assumed the presence of 3 distinguished isomers also for EHMPO and HMPPPO.

2.3. Hydroxyl radical adducts

The respective hydroxyl radical adducts were formed in an incubation system containing the respective spin traps (40 mM) together with an aqueous Fenton system^{20,21} (H_2O_2 (0.2%), EDTA (2 mM), and iron-(II) sulfate (1 mM)). The mixture was incubated

for a short period of time (ca. 10 s), then the reaction was stopped by 1:1 dilution with phosphate buffer (300 mM, pH 7.4; DTPA (20 mM)) and finally the mixture was rapidly transferred to an EPR flat cell and measured within the first 3 min. Figure 4a shows the respective spectrum obtained from the Fenton system with EHMPO. Two different species were formed, most probably corresponding to the diastereomeric forms of the spin adduct EHMPO/OH. Similarly, two isomers were detected from HMPPPO/OH (Fig. 4c) and HMiPPO/OH (Fig. 4d), whereas from EEHPO/OH (Fig. 4b) at least five different species contributed to the EPR spectrum, two of which showed HFS parameters similar to the adducts of the other three spin traps. The remaining contributions were difficult to identify, most probably being degradation products or species formed by hydroxyl radical attack to the hydroxymethyl side chain. The respective HFS data, obtained by computer simulation, are listed in Table 3. We also confirmed the identity of the respective OH-radical adducts nucleophilic addition of water (see

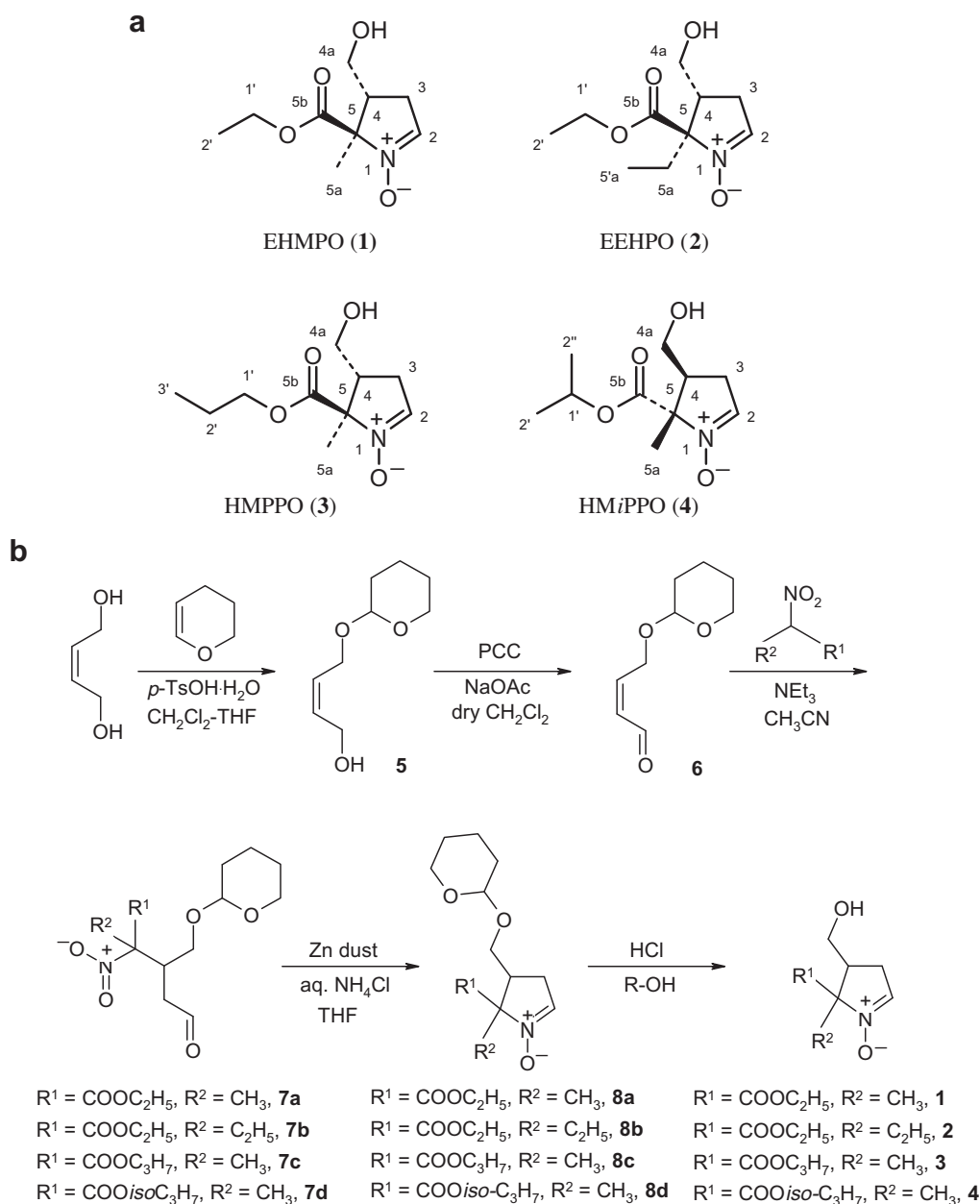


Figure 1. (a) General structure of the spin traps and (b) general synthetic scheme

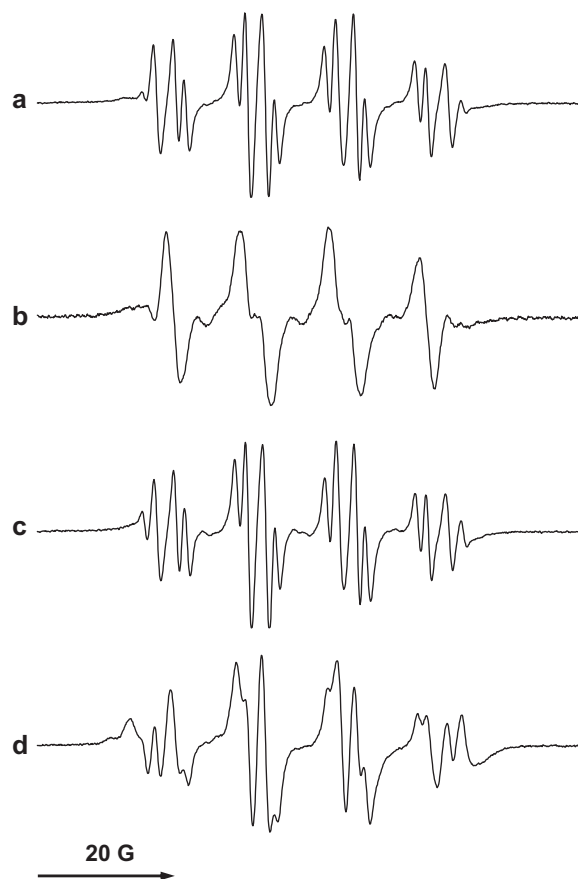


Figure 2. Superoxide radical spin adducts formed from EHMPO, EEHPO, HMPPPO and HMiPPO in a hypoxanthine/xanthine oxidase system. (a) EHMPO (20 mM) was dissolved in oxygenated phosphate buffer (20 mM, pH 7.4, containing 1 mM DTPA), catalase (250 U/mL), hypoxanthine (0.2 mM) and xanthine oxidase (150 mU/mL). After 7 min incubation maximum intensity was reached, SOD (150 units/mL) was added and a series of consecutive ESR spectra (every 90 s for 30 min) was recorded using the following EPR parameters: sweep width, 80 G; modulation amplitude, 0.74 G; microwave power, 20 mW; time constant, 0.08 s; receiver gain, 1×10^3 ; scan rate, 57.2 G/min, 1024 data points. (b) same as in (a) except that EEHPO (20 mM) was used. (c) same as in (a) except that HMPPPO (20 mM) was used same. (d) as in (a) except that HMiPPO (20 mM) was used.

Table 2
Half-life of the superoxide adducts

Compound	Apparent $t_{1/2}$ (min) (1st species)	Apparent $t_{1/2}$ (min) (2nd species)	Partition coefficient <i>n</i> -octanol/ phosphate buffer (100 mM, pH 7.0)
EMPO ^a	8.6	—	0.15
EHMPO	10.2	9.1	0.05
EEHPO	28.4	—	0.11
HMPPPO	9.8	9.0	0.15
HMiPPO	11.1	11.2	0.11

^a Data from Stolze et al. (2002)³

Supplementary data). Experiments performed under nitrogen did not show significant differences, except for slightly better spectral resolution (see Supplementary data).

2.4. Methyl radical adducts

We already reported the formation of methyl radical adducts with a series of EMPO derivatives,^{3–7} the radicals being formed in a modified aqueous Fenton system containing 20% DMSO.²⁰ After

brief incubation for several seconds, the reaction mixture was diluted 1:1 with phosphate buffer (300 mM, pH 7.4; 20 mM DTPA) and immediately measured. Two major components were formed of almost equal intensity. However, the satellite peaks found on either side of the central peak (rather short-lived with a_N ca. 15.5 G and a_H ca. 26.5 G, marked with asterisks) most probably originate from another spin adduct. A contribution of ¹³C satellite peaks can be excluded. Figure 5a shows the respective spin adduct EHMPO/CH₃, similar EPR spectra were found with EEHPO/CH₃ (Fig. 5b), HMPPPO/CH₃ (Fig. 5c), and HMiPPO/CH₃ (Fig. 5d). All EPR parameters were obtained by computer simulation and are listed in Table 3. Experiments performed under nitrogen did not show significant differences, except for slightly better spectral resolution (see Supplementary data).

2.5. Methanol-derived radical adducts

Similar Fenton systems^{20,21} were used to generate the $\cdot\text{CH}_2\text{OH}$ radical adducts, with DMSO being replaced by methanol. The EPR spectra of the adducts formed from EHMPO (Fig. 6a), EEHPO (Fig. 6c), HMPPPO (Fig. 6e), and HMiPPO (Fig. 6g) mainly consist of two almost equally intensive components with HFS parameters comparable to the respective methyl radical adducts (see Fig. 5). In addition, traces of a third species can be detected during the first few minutes. For comparison we also tried to synthesize the respective methoxyl radical adducts using the principle of ‘inverted spin trapping’, that is, nucleophilic addition of methanol to the spin trap in the presence of Fe³⁺, followed by oxidation to the radical adduct.²² However, the respective EPR spectra obtained from EHMPO (Fig. 6b), HMPPPO (Fig. 6f), and HMiPPO (Fig. 6h) show HFS values close to or even equal to the respective $\cdot\text{CH}_2\text{OH}$ adducts with additional secondary products being formed, none of them having the anticipated EPR parameters expected for the methoxyl adducts. From EEHPO (Fig. 6d) mostly the mixture of isomers of the $\cdot\text{CH}_2\text{OH}$ adducts were formed (56%) and about 8% of the CH₃O \cdot adduct was detected as a transient species for the first 3 min. In addition, about 36% of an unknown mixture of degradation products was detected. All EPR parameters were obtained by computer simulation and listed in Table 3. Experiments performed under nitrogen did not show significant differences, except for slightly better spectral resolution (see Supplementary data).

2.6. Ethanol-derived radical adducts

Similar Fenton systems^{20,21} were used in the presence of ethanol to generate the $\cdot\text{CH}(\text{CH}_3)\text{-OH}$ radical adducts. The EPR spectra obtained from EHMPO (Fig. 7a), EEHPO (Fig. 7c), HMPPPO (Fig. 7e), and HMiPPO (Fig. 7g) also consist of two major components as in the case of methanol-derived $\cdot\text{CH}_2\text{OH}$ radicals (see Fig. 6), as well as traces of a third, short-lived species. For comparison we also tried to synthesize the respective ethoxyl radical adducts in the presence of ethanol and Fe³⁺, followed by oxidation to the radical adduct.²² However, no ethoxyl adducts were found from EHMPO (Fig. 7b), HMPPPO (Fig. 7f), and HMiPPO (Fig. 7h), whereas with EEHPO (Fig. 7d) a complex mixture of different radicals was formed. Although involvement of the ethoxyl radical adduct cannot be excluded, a significant contribution seems, however, very unlikely. All EPR parameters were obtained by computer simulation and listed in Table 3. Experiments performed under nitrogen did not show significant differences, except for slightly better spectral resolution (see Supplementary data).

2.7. Formate-derived radical adducts

Similarly, the use of an aqueous sodium formate solution (200 mM) under otherwise identical conditions lead to the

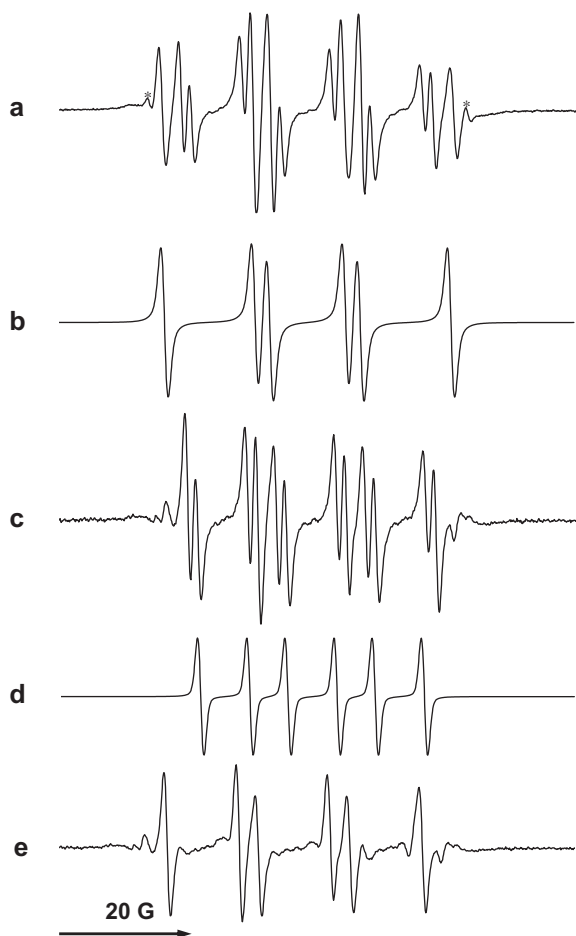


Figure 3. Simulation of the spectrum of the EHMPO superoxide adduct. (a) whole spectrum (see also Fig. 2a). (b) simulation of the first species ($a_N = 13.64$; $a_H = 15.88$; 50%). (c) difference spectrum (simulation #1 subtracted from original spectrum shown in Fig. 3a). (d) simulation of the second species ($a_N = 13.36$; $a_H = 7.54$; 25%). (e) difference spectrum (simulation #2 subtracted from the spectrum shown in Fig. 3c) (simulation #3: $a_N = 13.36$; $a_H = 10.50$; 25%).

formation of the respective carbon dioxide anion radical adducts.^{20,21} The characteristic ESR spectra are shown in Figure 8a (EHMPO/ CO_2^-), Figure 8b (EEHPO/ CO_2^-), Figure 8c (HMPPPO/ CO_2^-), and Figure 8d (HMiPPO/ CO_2^-). From EHMPO and HMiPPO four different products were formed and three from HMMPO. A distinct carbon dioxide anion radical adduct as a predominant major species (72%) was detectable with EEHPO (Fig. 8b), together with traces of a secondary species having a ten times lower concentration (7%). In addition, about 21% of the hydroxyl radical adduct (mixture of isomers) was also detectable. The HFS data are listed in Table 3. Experiments performed under nitrogen did not show significant differences, except for slightly better spectral resolution (see Supplementary data).

2.8. Radical adducts formed upon reduction of the spin traps

Upon reduction of the respective spin traps with KBH_4 , the formation of pseudo- H^\cdot adducts was observed. The results are shown in Figure 9a (EHMPO/ H^\cdot), Figure 9b (EEHPO/ H^\cdot), Figure 9c (HMPPPO/ H^\cdot), and Figure 9d (HMiPPO/ H^\cdot). In all cases two major components were formed, which could only be calculated by computer simulation (asymmetric form of the lines due to two different isomers hidden within the spectral line width). Synthesis of the adducts was performed by addition of a small amount of KBH_4 (ca. 0.5 mg/500 μl) to the respective spin trap (40 mM),

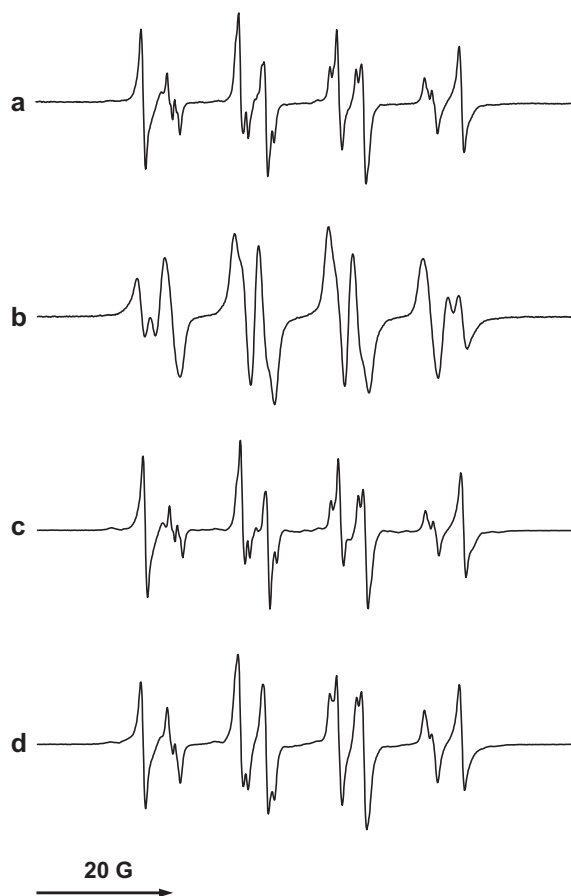


Figure 4. Iron-dependent formation of hydroxyl radical spin adducts from EHMPO, EEHPO, HMPPPO and HMiPPO. (a) EHMPO (40 mM, initial concentration) was incubated with a Fenton system containing FeSO_4 (1 mM), EDTA (2 mM), H_2O_2 (0.2%). The reaction was stopped after 10 s by 1:1 dilution with phosphate buffer (300 mM, pH 7.4, containing 20 mM DTPA) and the spectrum was recorded using the following spectrometer settings: sweep width, 80 G; modulation amplitude, 0.1 G; microwave power, 20 mW; time constant, 0.08 s; receiver gain, 5×10^3 ; scan rate, 57.2 G/min, 1024 data points. (b) same as in a), except that EEHPO was used (gain 1×10^4 , modulation amplitude, 0.2 G). (c) same as in a), except that HMPPPO was used (gain 1×10^4 , modulation amplitude, 0.2 G). (d) same as in a), except that HMiPPO was used (gain 1×10^4 , modulation amplitude, 0.2 G).

followed by readjusting of the pH to 7.4 by 1:1 dilution with phosphate buffer (300 mM, pH 7.4, containing 20 mM DTPA), which led to the observation of the respective H^\cdot adducts. If necessary, a small amount of $\text{K}_3[\text{Fe}(\text{CN})_6]$ was added to prevent reduction of the spin adducts due to excess of KBH_4 . All EPR parameters as obtained by computer simulation are listed in Table 3.

3. Discussion

Four novel spin traps were synthesized in this study, all of which being 5-alkoxycarbonyl-5-alkylpyrroline N-oxide (EMPO) derivatives with an additional hydroxymethyl substituent in position 4 of the pyrroline ring. The chemical structure of the compounds was assessed by full NMR assignment (^1H and ^{13}C), FTIR, and UV–vis spectroscopy, and the purity by MS analysis and microanalysis. The spin trapping properties as well as the EPR parameters of the respective spin adducts were studied and compared with the parent compound EMPO.^{3–7}

Modification of the spin trap with an additional group, such as hydroxyl or amino functionalities, permits rapid subsequent structural modification under relatively mild conditions which even leave the labile nitron moiety unaffected. Such subsequent

Table 3
Comparison of the EPR parameters of different radical adducts of EMPO, EHMPPO, EEHPO, HMPPPO, and HMiPPPO

Radical	HFS EMPO ^a (G)	EHMPPO				EEHPO				HMPPPO			HMiPPPO		
·OOH	trans ^b (94%) ^c	cis ^b (6%)				(50%)				(50%)			(50%)		
	a ^N	13.27	13.25	13.25	13.64	13.36	13.36	13.20	13.14	13.60	13.34	13.34	13.37	13.37	13.65
	a ^H	12.37	9.30	10.15	15.88	10.50	7.54	11.90	9.77	15.89	10.52	7.52	11.16	8.42	15.90
	a ^H (55.5%/ 44.5% of trans ^{b,c})	1.50	—	—	—	—	—	—	—	—	—	—	—	—	—
·OH	trans** (76%)	cis** (24%)				(60%)				(40%)			(48%)		
	a ^N	14.11	14.18	14.50	13.98	13.87	14.00	14.47	15.47	14.05	14.45	13.93	14.45	13.98	
	a ^H	12.80	15.27	18.10	10.15	11.44	8.96	18.60	16.60	15.95	18.18	10.00	18.27	10.15	
	a ^H	0.63	0.62	0.23	1.05	—	—	—	—	—	0.20	1.08	0.26	1.05	
	a ^H	0.43	0.50	—	0.45	—	—	—	—	—	—	0.47	—	0.45	
	a ^H 0.21 ⁽³⁾	0.21 ⁽³⁾	—	—	—	—	—	—	—	—	—	—	—	—	
a ^H 0.13 ²	0.07 ⁽²⁾	—	—	—	—	—	—	—	—	—	—	—	—		
·H	(100%)	(84 %)				(16%)				(50 %)			(50%)		
	a ^N	15.52	15.55	15.05	15.20	15.20	15.58	15.58	15.58	15.58	15.58	15.58	15.58	15.58	
	a ^H	22.21	25.33	21.40	24.83	24.83	25.40	25.40	25.40	25.40	25.40	25.40	25.40	25.12	
	a ^H	20.82	17.50	20.60	19.30	16.90	17.92	16.82	17.41	18.42	—	—	—	—	
·CH ₃	(100%)	(52 %)				(48%)				(50%)			(61 %)		
	a ^N	15.42	15.26	15.43	15.02	15.02	15.44	15.21	15.22	15.50	—	—	—	—	
	a ^H	22.30	17.94	17.94	19.15	17.25	17.67	17.67	17.90	17.70	—	—	—	—	
	a ^H	—	0.37 ⁽⁴⁾	0.37 ⁽⁴⁾	—	—	—	0.36 ⁽⁴⁾	0.36 ⁽⁴⁾	0.37 ⁽⁴⁾	—	—	—	—	
MeOH/Fe ³⁺	(50%)	(50%)	(71%)	(29%)	(56%)	(8%)	(36%) ^d	(66%)	(34%)	(82%)	(18%)	—	—	—	
	a ^N	13.74	13.74	15.01	15.01	14.61	13.41	—	14.96	15.00	14.97	15.01	—	—	
	a ^H	10.87	7.81	17.87	25.25	18.60	7.00	—	17.61	25.23	18.02	25.21	—	—	
	a ^H	—	—	(0.60)	(0.60)	(0.87/0.5)	1.20	—	(0.53 ²)	(0.60)	(.59/ .50)	(0.60)	—	—	
·CH ₂ OH	(100%)	(52%)				(48%)				(50%)			(50%)		
	a ^N	14.95	15.10	14.96	14.63	14.63	15.02	14.96	14.98	14.94	—	—	—	—	
	a ^H	21.25	17.75	17.75	19.55	17.81	17.61	17.61	17.81	17.81	—	—	—	—	
	a ^H	—	0.52 ⁽²⁾	0.52 ⁽²⁾	0.50	0.50	0.53 ⁽²⁾	0.53 ⁽²⁾	0.55 ⁽²⁾	0.55 ⁽²⁾	—	—	—	—	
EtOH/Fe ³⁺	—	(88%)				(12%)				(58%)			(35%)		
	a ^N	—	15.02	15.01	14.52	13.30	15.06	15.01	14.95	15.01	15.15	—	—	—	
	a ^H	—	18.33	25.25	19.20	7.84	(0.50)	18.19	25.30	18.31	25.04	—	—	—	
	a ^H	—	(0.57 ²)	(0.60)	(.9/.5)	(.9 ² /.5)	—	(.64/.50)	(.64/.50)	(.55 ² / .40 ²)	(0.57 ²)	—	—	—	
·CH(OH)CH ₃	(67%)	(33%)	(50%)	(50%)	(50%)	(50%)			(50%)			(50%)			
	a ^N	14.94	15.00	15.06	14.95	14.64	14.50	15.07	14.94	15.07	14.95	—	—	—	
	a ^H	20.82	22.40	18.33	18.53	19.13	19.45	18.15	18.38	18.30	18.54	—	—	—	
	a ^H	—	—	0.57 ⁽²⁾	0.57 ⁽²⁾	0.85 ⁽²⁾	0.85 ⁽²⁾	0.64	0.64	0.55	0.55	—	—	—	
·CO ₂ ⁻	(100%)	(34%)				(30%)				(22%)			(14%)		
	a ^N	14.74	15.05	13.95	14.82	15.08	14.58	14.70	15.05	14.83	15.08	14.87	14.90	14.98	
	a ^H	17.16	16.73	16.78	23.15	15.66	17.31	24.22	16.83	23.13	15.74	15.26	16.15	16.98	
	—	—	0.25	0.40	0.45	—	0.55	0.45	—	0.43	—	0.23	—	0.43	

^a Data from Stolze et al.^{3,7}

^b Data from Culcasi et al.²³

^c Mixture of rotamers.

^d Mixture of secondary products.

^e Mixture of hydroxyl radical adduct and other secondary products.

alterations might be used to direct the spin trap to specific areas or organelles.

One limitation of the spin trapping technique in biological systems is the biochemical reduction of the spin trap within cells and mitochondria. Also, the lower rate of spin trapping compared to other analytical techniques is a serious limitation. Compared to other EPR techniques spin trapping is slower than detection of radicals using 'spin probes' (e.g., CPH, 1-hydroxy-3-carboxy-2,2,5,5-tetramethylpyrrolidine), but gives more information about the radical trapped. Therefore, spin trapping always has to be used in combination with other analytical techniques.

A typical characteristic of substituted spin traps is the presence of two or more chiral carbon centers, thereby causing the formation of at least two different diastereomers of the investigated spin

traps. Addition of radicals from the two different stereofaces eventually produces two additional stereocenters at C-2 having similar, but not identical EPR parameters, and the respective adducts therefore cannot always be clearly distinguished. Furthermore, free radicals can also attack the hydroxymethyl side chain, thereby generating secondary radicals which, with a second molecule of spin trap, react to a variety of secondary spin adducts.

The stabilities of the respective superoxide adducts were very promising, that is, similar to the parent compound EMPO or even higher, although the adducts were not as stable as those of the respective DEPMPO derivatives.^{8–10} On the other hand, the present synthesis of 4-hydroxymethyl derivatives of the EMPO series is more straightforward and less complicated compared to the respective DEPMPO compound.

All spin traps were forming characteristic hydroxyl radical adducts. Methoxyl radical adducts were rather unstable and could not be detected in neat form: the hydroxymethyl radical adducts were always dominating the EPR spectra. Rather stable spin adducts were formed from carbon-centered radicals, generated in Fenton systems in the presence of DMSO ($\cdot\text{CH}_3$), methanol ($\cdot\text{CH}_2\text{OH}$), ethanol ($\cdot\text{CH}(\text{CH}_3)\text{OH}$), and formate ($\cdot\text{CO}_2^-$).

4. Conclusion

In conclusion, all four novel EMPO-derived spin traps formed reasonably stable superoxide adducts ($t_{1/2}$ ca. 8–30 min) and are therefore also suitable for superoxide trapping in biological systems. They are also advantageous for the detection of carbon-centered radicals. The compounds are good candidates for modification with site-directing groups (e.g., by ester formation at the 4-hydroxymethyl group), which will be the topic of a forthcoming report.

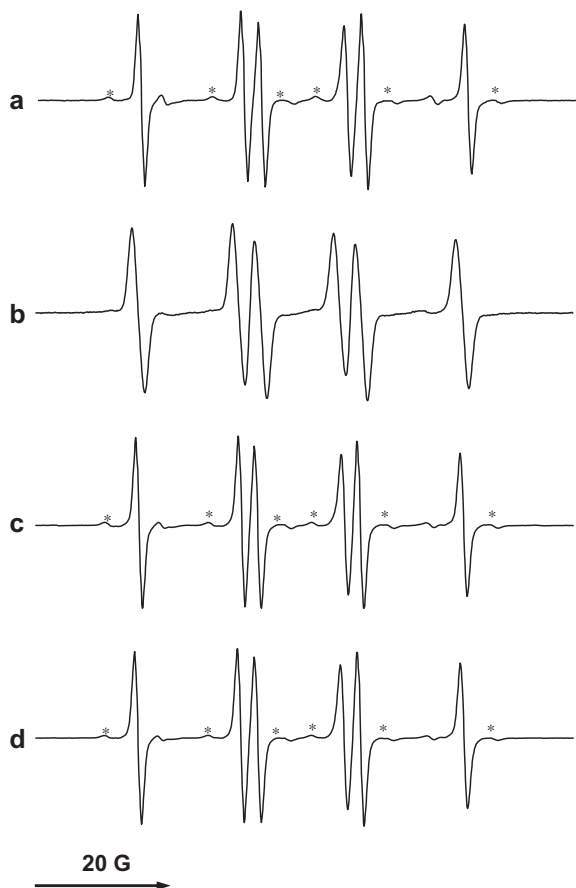


Figure 5. Iron-dependent formation of methyl radical spin adducts from EHMPO, EEHPO, HMPPPO and HMiPPO in the presence of DMSO. (a) EHMPO (40 mM, initial concentration) was incubated with a Fenton system containing FeSO_4 (1 mM), EDTA (2 mM), H_2O_2 (0.2%) in 20% DMSO. The reaction was stopped after 10 s by 1:1 dilution with phosphate buffer (300 mM, pH 7.4, containing 20 mM DTPA) and the spectrum was recorded using the following spectrometer settings: sweep width, 80 G; modulation amplitude, 0.1 G; microwave power, 20 mW; time constant, 0.08 s; receiver gain, 5×10^3 ; scan rate, 57.2 G/min, 1024 data points. (b) same as in a), except that EEHPO was used (gain 1×10^4 , modulation amplitude, 0.2 G). (c) same as in a), except that HMPPPO was used (gain 1×10^4 , modulation amplitude, 0.2 G). (d) same as in a), except that HMiPPO was used (gain 1×10^4 , modulation amplitude, 0.2 G).

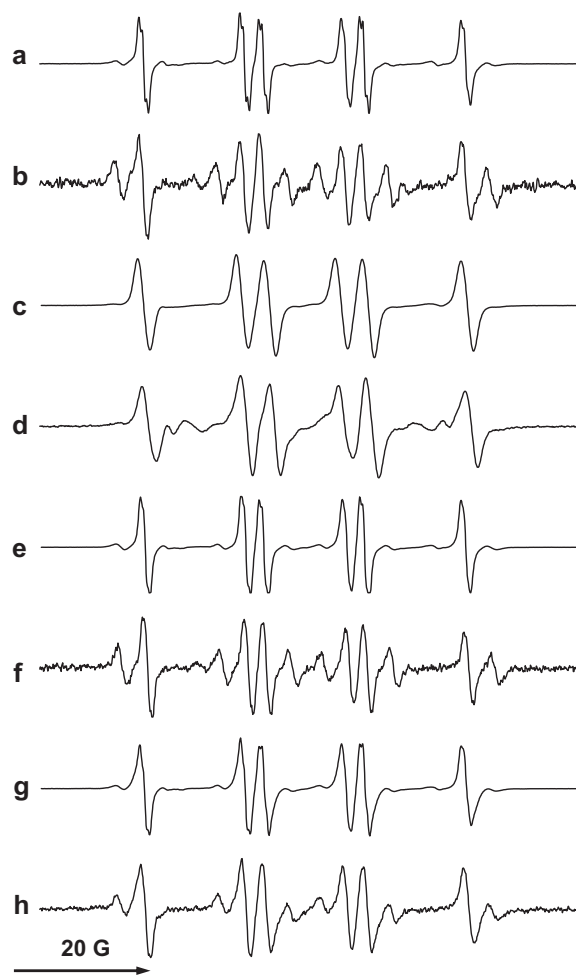


Figure 6. Iron-dependent formation of methanol-derived radical spin adducts from EHMPO, EEHPO, HMPPPO and HMiPPO. (a) EHMPO (40 mM, initial concentration) was incubated with a Fenton system containing FeSO_4 (1 mM), EDTA (2 mM), H_2O_2 (0.2%) in 20% methanol. The reaction was stopped after 10 s by 1:1 dilution with phosphate buffer (300 mM, pH 7.4, containing 20 mM DTPA) and the spectrum was recorded using the following spectrometer settings: sweep width, 80 G; modulation amplitude, 0.1 G; microwave power, 20 mW; time constant, 0.08 s; receiver gain, 5×10^3 ; scan rate, 57.2 G/min. (b) After a 30 s incubation of EHMPO (1 M in methanol) with FeCl_3 (10 mM), the reaction was stopped by 1:20 dilution with phosphate buffer (0.3 M, pH 7.4, containing 20 mM DTPA), and the spectrum was recorded with the following spectrometer settings: sweep width, 80 G; modulation amplitude, 0.5 G; microwave power, 20 mW; time constant, 0.02 s; receiver gain, 5×10^4 ; scan rate, 229 G/min, 1024 data points. (c) same as in a), except that EEHPO was used (gain 1×10^4 , modulation amplitude, 0.2 G). (d) same as in b), except that EEHPO was used. (e) same as in a), except that HMPPPO was used (gain 1×10^4 , modulation amplitude, 0.2 G). (f) same as in b), except that HMPPPO was used. (g) same as in a), except that HMiPPO was used (gain 1×10^4 , modulation amplitude, 0.2 G). (h) same as in b), except that HMiPPO was used.

5. Experimental

5.1. Chemicals

Ethyl-2-nitropropanoate was from Alfa Aesar, pyridinium chlorochromate and triethylamine were from Fluka, *p*-toluenesulfonic acid monohydrate, and 3,4-dihydro-(2*H*)-pyrane were from Sigma-Aldrich, all other chemicals were obtained from VWR. All reactions were performed in oven-dried glassware under dry argon atmosphere. CH_2Cl_2 was freshly distilled from CaH_2 under argon. Column chromatography was carried out with SiO_2 60 (particle size 0.040–0.063 mm, 230–400 mesh; Merck) and commercially available solvents. Thin-layer chromatography (TLC) was

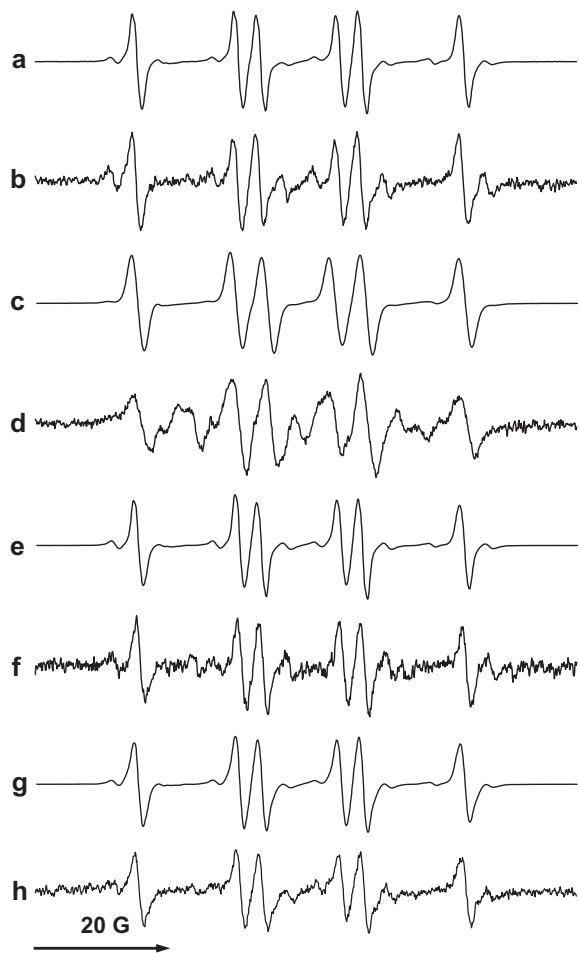


Figure 7. Iron-dependent formation of ethanol-derived radical spin adducts from EHMPO, EEHPO, HMPPPO and HMiPPPO. (a) EHMPO (40 mM, initial concentration) was incubated with a Fenton system containing FeSO_4 (1 mM), EDTA (2 mM), H_2O_2 (0.2%) in 20% ethanol. The reaction was stopped after 10 s by 1:1 dilution with phosphate buffer (300 mM, pH 7.4, containing 20 mM DTPA) and the spectrum was recorded using the following spectrometer settings: sweep width, 80 G; modulation amplitude, 0.1 G; microwave power, 20 mW; time constant, 0.08 s; receiver gain, 5×10^3 ; scan rate, 57.2 G/min, 1024 data points. (b) After a 30 s incubation of EHMPO (1 M in ethanol) with FeCl_3 (10 mM), the reaction was stopped by 1:20 dilution with phosphate buffer (0.3 M, pH 7.4, containing 20 mM DTPA), and the spectrum was recorded with the following spectrometer settings: sweep width, 80 G; modulation amplitude, 0.5 G; microwave power, 20 mW; time constant, 0.02 s; receiver gain, 5×10^4 ; scan rate, 229 G/min, 1024 data points. (c) same as in (a), except that EEHPO was used (gain 1×10^4 , modulation amplitude, 0.2 G). (d) same as in (b), except that EEHPO was used. (e) same as in (a), except that HMPPPO was used (gain 1×10^4 , modulation amplitude, 0.2 G). (f) same as in (b), except that HMPPPO was used. (g) same as in (a), except that HMiPPPO was used (gain 1×10^4 , modulation amplitude, 0.2 G). (h) same as in (b), except that HMiPPPO was used.

conducted on silica 60-coated glass plates from Merck, with visualization either by UV light (254 or 360 nm), *p*-anisaldehyde or ninhydrine spray reagents.

^1H and ^{13}C NMR spectra were recorded in CDCl_3 at 400 and 100 MHz for ^1H and ^{13}C , respectively, at a Bruker AVANCE II instrument. Chemical shifts are reported in ppm relative to the signal of Me_4Si . Coupling constants (J) are given in Hz. CDCl_3 was used as the solvent if not otherwise stated. The apparent resonance multiplicity is described as s (singlet), br s (broad singlet), d (doublet), dd (doublet of doublet), t (triplet), q (quartet) and m (multiplet). Additional NMR techniques such as APT (attached proton test), ^1H , ^1H COSY, HMBC (heteronuclear multiple bond connectivity) and HMQC (^1H -detected heteronuclear multiple-quantum coherence) were used for signal assignment. The mass spectra were measured

on a ESI Q-TOF MS on a waters Micromass Q-TOF Ultima Global in 70% aqueous methanol containing 0.1% formic acid at a flow rate of 5 $\mu\text{l}/\text{min}$. IR spectra were recorded as film on an ATI Mattson Genesis Series FT-IR spectrometer. UV-vis spectra were recorded on a Hitachi 150-20 and U-3300 spectrophotometers in double-beam mode against a blank of the respective solvent. Determination of the concentrations was done measuring the absorption maxima in the range between 200 and 300 nm. For measurements of the partition coefficients, 500 μl of *n*-octanol was added to 500 μl of a solution of the respective spin trap (100 mM or 5–10 mg, respectively) in 100 mM phosphate buffer, pH 7.4. The mixture was vortexed for 2 min at room temperature. If necessary, the procedure was repeated several times, until an equilibrium between the two phases was achieved. After careful separation of the phases, the absorbance was read at the maximum around 235 nm after dilution with methanol. For EPR experiments, Bruker spectrometers (ESP300E and EMX) were used, operating at 9.7 GHz with 100 kHz modulation frequency, equipped with a rectangular TE_{102} or a TM_{110} microwave cavity. All calculations for spectral simulation were done using the SimFonia Program by Bruker.

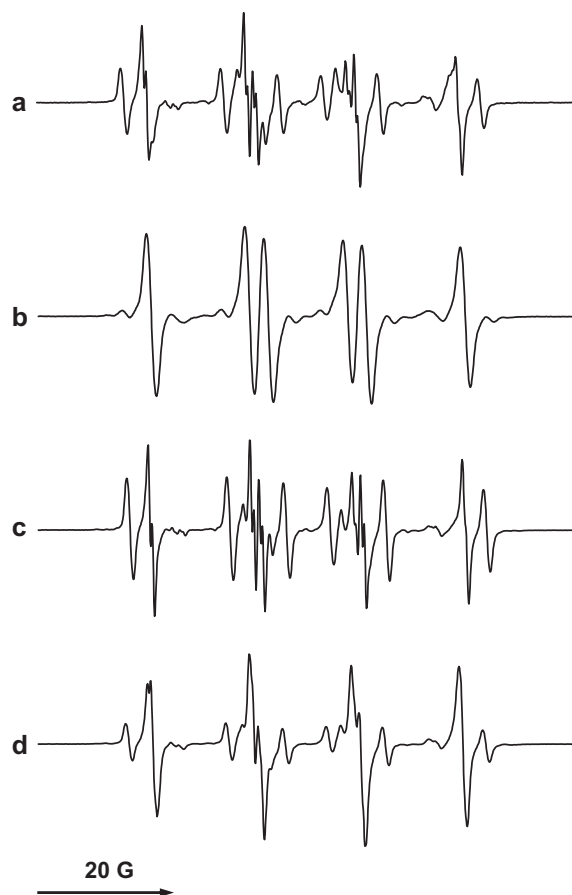


Figure 8. Iron-dependent formation of carbon-centered spin adducts from EHMPO, EEHPO, HMPPPO and HMiPPPO in the presence of formate. (a) EHMPO (40 mM, initial concentration) was incubated with a Fenton system containing FeSO_4 (1 mM), EDTA (2 mM), H_2O_2 (0.2%) and sodium formate (200 mM). The reaction was stopped after 10 s by 1:1 dilution with phosphate buffer (300 mM, pH 7.4, containing 20 mM DTPA) and the spectrum was recorded using the following spectrometer settings: sweep width, 80 G; modulation amplitude, 0.1 G; microwave power, 20 mW; time constant, 0.08 s; receiver gain, 5×10^3 ; scan rate, 57.2 G/min, 1024 data points. (b) same as in (a), except that EEHPO was used (gain 1×10^4 , modulation amplitude, 0.2 G). (c) same as in (a), except that HMPPPO was used (gain 1×10^4 , modulation amplitude, 0.2 G). (d) same as in (a), except that HMiPPPO was used (gain 1×10^4 , modulation amplitude, 0.2 G).

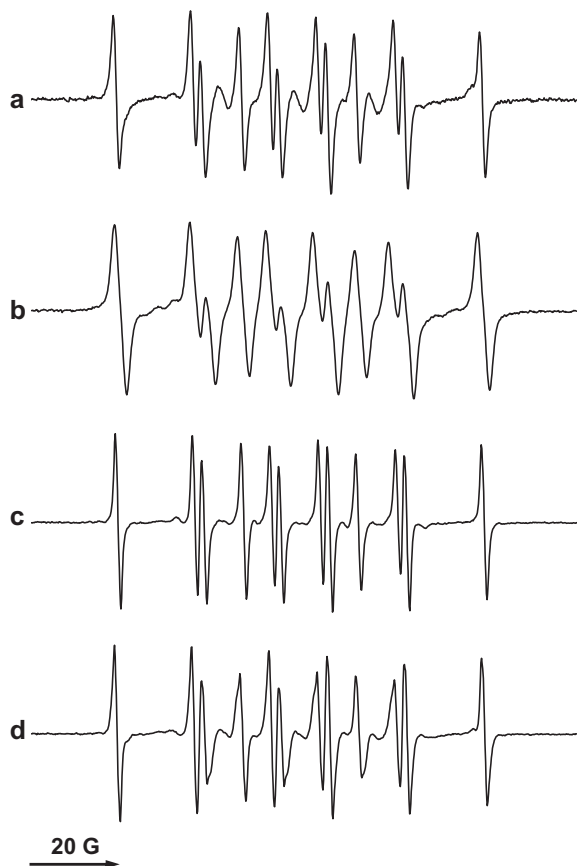


Figure 9. Formation of hydrogen spin adducts (reduction products) from EHMPO, EEHPO, HMPPPO and HMiPPPO and KBH_4 . (a) EHMPO (50 mM, initial concentration) was incubated with approximately 1 mg KBH_4 for 1 min, then EDTA (2 mM) was added, the solution was diluted 1:1 with phosphate buffer (300 mM, pH 7.4, containing 20 mM DTPA), a few drops of a $\text{K}_3\text{Fe}(\text{CN})_6$ solution were added until the mixture remained slightly yellow and the spectrum was recorded using the following spectrometer settings: sweep width, 120 G; modulation amplitude, 0.1 G; microwave power, 20 mW; time constant, 0.08 s; receiver gain, 5×10^3 ; scan rate, 86 G/min, 1024 data points. (b) same as in a), except that EEHPO was used (gain 1×10^4 , modulation amplitude, 0.2 G). (c) same as in a), except that HMPPPO was used (gain 1×10^4 , modulation amplitude, 0.2 G). (d) same as in a), except that HMiPPPO was used (gain 1×10^4 , modulation amplitude, 0.2 G).

5.1.1. 5-Ethoxycarbonyl-4-hydroxymethyl-5-methyl-pyrroline N-oxide (EHMPO)

Column chromatography: gradient $\text{CH}_2\text{Cl}_2 \rightarrow \text{CH}_2\text{Cl}_2/\text{MeOH}$ ($v/v = 99:1$), colorless oil, color reaction with ninhydrine reagent: green. $R_f = 0.20$ ($\text{CH}_2\text{Cl}_2/\text{MeOH}$, $v/v = 9:1$). ^1H NMR: δ 1.29 (3H, t, 2°CH_3), 1.64 (3H, s, 5^aCH_3), 2.45–3.51 (1H, ddd, 3°CH_2), 2.79–2.87 (1H, ddd, 3°CH_2), 3.04 (1H, m, 4°CH), 3.66–3.78 (2H, m, 4^aCH_2), 4.19–4.32 (2H, m, 1°CH_2), 6.92 (1H, t, 2°CH). ^{13}C NMR: δ 14.00 (2°CH_3), 14.85 (5^aCH_3), 29.78 (3°CH_2), 43.79 (4°CH), 61.34 (1°CH_2), 62.61 (4^aCH_2), 81.17 (5°C), 134.83 (2°CH), 170.07 (5^bC). Anal. Calcd. for $\text{C}_9\text{H}_{15}\text{O}_4\text{N}_1$ (201.22): C 53.72, H 7.51, N 6.96; found: C 53.70, H 7.52, N, 6.90. HRMS calcd for $\text{C}_9\text{H}_{15}\text{O}_4\text{N}_1$ [$\text{C}_9\text{H}_{15}\text{O}_4\text{N}_1 + \text{H}$] $^+$: 202.22. Found: 202.22.

5.1.2. 5-Ethoxycarbonyl-5-ethyl-4-hydroxymethyl-pyrroline N-oxide (EEHPO)

Column chromatography: gradient $\text{CH}_2\text{Cl}_2 \rightarrow \text{CH}_2\text{Cl}_2/\text{MeOH}$ ($v/v = 99:1$), color reaction with ninhydrine reagent: green. $R_f = 0.24$ ($\text{CH}_2\text{Cl}_2/\text{MeOH}$, $v/v = 9:1$), colorless oil. ^1H NMR: δ 1.29 (3H, t, 2°CH_3), 1.64 (3H, s, 5^aCH_3), 2.45–3.51 (1H, ddd, 3°CH_2), 2.79–2.87 (1H, ddd, 3°CH_2), 3.04 (1H, m, 4°CH), 3.66–3.78 (2H, m, 4^aCH_2), 4.19–4.32 (2H, m, 1°CH_2), 6.92 (1H, t, 2°CH). ^{13}C NMR: 8.22 (5^aCH_3), 13.19 (2°CH_3), 22.00 (5^aCH_2), 29.98 (3°CH_2), 43.51 (4°CH), 60.00

(1°CH_2), 62.00 (4^aCH_2), 83.25 (5°C), 134.13 (2°CH), 169.07 (5^bC). Anal. Calcd. for $\text{C}_{10}\text{H}_{17}\text{O}_4\text{N}_1$ (215.24): C 55.80, H 7.96, N 6.51; found: C 55.75, H 7.93, N, 6.56. HRMS calcd for $\text{C}_{10}\text{H}_{17}\text{O}_4\text{N}_1$ [$\text{C}_{10}\text{H}_{17}\text{O}_4\text{N}_1 + \text{H}$] $^+$: 216.24. Found: 216.24.

5.1.3. 4-Hydroxymethyl-5-methyl-5-propoxycarbonyl-pyrroline N-oxide (HMPPPO)

Column chromatography: gradient $\text{CH}_2\text{Cl}_2 \rightarrow \text{CH}_2\text{Cl}_2/\text{MeOH}$ ($v/v = 99:1$), color reaction with ninhydrine reagent: green. $R_f = 0.26$ ($\text{CH}_2\text{Cl}_2/\text{MeOH}$, $v/v = 9:1$), colorless oil. ^1H NMR: δ 0.94 (3H, t, 3°CH_3), 1.60 (3H, s, 5^aCH_3), 1.70–1.76 (2H, m, 2°CH_2), 2.42–2.56 (1H, m, 3°CH_2), 2.76–2.91 (1H, m, 3°CH_2), 2.93–3.06 (1H, m, 4°CH), 3.64–3.80 (2H, m, 4^aCH_2), 4.10–4.21 (2H, m, 1°CH_2), 6.92 (1H, t, 2°CH). ^{13}C NMR: δ 10.61 (3°CH_3), 14.65 (5^aCH_3), 21.88 (2°CH_2), 29.80 (3°CH_2), 44.11 (4°CH), 61.45 (4^aCH_2), 68.01 (1°CH_2), 81.31 (5°C), 135.01 (2°CH), 170.36 (5^bC). Anal. Calcd. for $\text{C}_{10}\text{H}_{17}\text{O}_4\text{N}_1$ (215.24): C 55.80, H 7.96, N 6.51; found: C 55.79, H 7.95, N 6.52. HRMS calcd for $\text{C}_{10}\text{H}_{17}\text{O}_4\text{N}_1$ [$\text{C}_{10}\text{H}_{17}\text{O}_4\text{N}_1 + \text{H}$] $^+$: 216.24. Found: 216.24.

5.1.4. 4-Hydroxymethyl-5-methyl-5-iso-propoxycarbonyl-pyrroline N-oxide (HMiPPPO)

Column chromatography: gradient $\text{CH}_2\text{Cl}_2 \rightarrow \text{CH}_2\text{Cl}_2/\text{MeOH}$ ($v/v = 99:1$), color reaction with ninhydrine reagent: green, $R_f = 0.26$ ($\text{CH}_2\text{Cl}_2/\text{MeOH}$, $v/v = 9:1$), colorless oil. ^1H NMR: δ 1.22 (6H, d, $2^\circ, 2^\circ\text{CH}_3$), 1.58 (3H, s, 5^aCH_3), 2.42–3.53 (1H, m, 3°CH_2), 2.73–2.87 (1H, m, 3°CH_2), 2.87–2.95 (1H, m, 4°CH), 3.56–3.72 (2H, m, 4^aCH_2), 4.96–5.08 (1H, m, 1°CH), 6.91 (1H, t, 2°CH). ^{13}C NMR: δ 14.54 (5^aCH_3), 21.47 ($2^\circ, 2^\circ\text{CH}_3$), 29.95 (3°CH_2), 43.81 (4°CH), 61.12 (4^aCH_2), 70.15 (1°CH), 81.09 (5°C), 135.92 (2°CH), 169.34 (5^bC). Anal. Calcd. for $\text{C}_{10}\text{H}_{17}\text{O}_4\text{N}_1$ (215.24): C 55.80, H 7.96, N 6.51; found: C 55.76, H 7.98, N 6.50. HRMS calcd for $\text{C}_{10}\text{H}_{17}\text{O}_4\text{N}_1$ [$\text{C}_{10}\text{H}_{17}\text{O}_4\text{N}_1 + \text{H}$] $^+$: 216.24. Found: 216.23.

Acknowledgments

The authors thank Christian-Doppler Society for financial support of this investigation, Dr. Andreas Hofinger for NMR measurements, and Mr. Philipp Jodl for skilful technical assistance in synthesis, purification, and characterization of the spin traps.

Supplementary data

Supplementary data (experimental procedures and spectra (^1H , ^{13}C (APT), COSY, HMBC, HMQC, NOESY) of the products) associated with this article can be found, in the online version, at doi:10.1016/j.bmc.2011.10.017.

References and notes

- Fréjaville, C.; Karoui, H.; Tuccio, B.; Le Moigne, F.; Culcasi, M.; Pietri, S.; Lauricella, R.; Tordo, P. *J. Med. Chem.* **1995**, *38*, 258.
- Stolze, K.; Udilova, N.; Nohl, H. *Free Radical Biol. Med.* **2000**, *29*, 1005.
- Stolze, K.; Udilova, N.; Nohl, H. *Biol. Chem.* **2002**, *383*, 813.
- Stolze, K.; Udilova, N.; Rosenau, T.; Hofinger, A.; Nohl, H. *Biol. Chem.* **2003**, *384*, 493.
- Stolze, K.; Rohr-Udilova, N.; Rosenau, T.; Stadtmüller, R.; Nohl, H. *Biochem. Pharmacol.* **2005**, *69*, 1351.
- Stolze, K.; Rohr-Udilova, N.; Rosenau, T.; Hofinger, A.; Kolarich, D.; Nohl, H. *Bioorg. Med. Chem.* **2006**, *14*, 3368.
- Stolze, K.; Rohr-Udilova, N.; Rosenau, T.; Hofinger, A.; Nohl, H. *Bioorg. Med. Chem.* **2007**, *15*, 2827.
- Hardy, M.; Chalier, F.; Ouari, O.; Finet, J.-P.; Rockenbauer, A.; Tordo, P. *Chem. Commun.* **2007**, 1083.
- Chalier, F.; Hardy, M.; Ouari, O.; Rockenbauer, A.; Tordo, P. *J. Org. Chem.* **2007**, *72*, 7886.
- Hardy, M.; Rockenbauer, A.; Vasquez-Vivar, J.; Felix, C.; Lopez, M.; Srinivasan, S.; Avadhani, N.; Tordo, Paul.; Kalyanaraman, B. *Chem. Res. Toxicol.* **2007**, *20*, 1053.
- Stolze, K.; Rohr-Udilova, N.; Patel, A.; Rosenau, T. *Bioorg. Med. Chem.* **2011**, *19*, 985–993.

12. Zhang, H.; Joseph, J.; Vasquez-Vivar, J.; Karoui, H.; Nsanzumuhire, C.; Martásek, P.; Tordo, P.; Kalyanaraman, B. *FEBS Lett.* **2000**, *473*, 58.
13. Olive, G.; Mercier, A.; LeMoigne, F.; Rockenbauer, A.; Tordo, P. *Free Radical Biol.Med.* **2000**, *28*, 403.
14. Deslongchamps, P.; Lamothe, S.; Lin, H.-S. *Can. J. Chem.* **1987**, *65*, 1298–1307. "A simple and direct method of cyclization for the synthesis of 10-membered rings".
15. Corey, E. J.; Suggs, J. W. *Tetrahedron. Lett.* **1975**, *31*, 2647–2650. "Pyridinium chlorochromate. An efficient reagent for oxidation of primary and secondary alcohols to carbonyl compounds".
16. Tsai, P.; Ichikawa, K.; Mailer, C.; Pou, S.; Halpern, H. J.; Robinson, B.; Nielsen, R.; Rosen, G. M. *J. Org. Chem.* **2003**, *68*, 7811–7817. "Esters of 5-carboxy-5-methyl-1-pyrroline N-oxide: A family of spin traps for superoxide".
17. Karoui, H.; Clément, J.-L.; Rockenbauer, A.; Siri, D.; Tordo, P. *Tetrahedron Lett.* **2004**, *45*, 149–152. "Synthesis and structure of 5,5-diethoxycarbonyl-1-pyrroline-N-oxide (DECPO). Application to superoxide radical trapping".
18. Nsanzumuhire, C.; Clément, J.-L.; Ouari, O.; Karoui, H.; Finet, J.-P.; Tordo, P. *Tetrahedron Lett.* **2004**, *45*, 6385–6389. "Synthesis of the cis diastereoisomer of 5-diethoxyphosphoryl-5-methyl-3-phenyl-1-pyrroline N-oxide (DEPMPPoc) and ESR study of its superoxide spin adduct".
19. Sergey Dikalov, Jinjie Jiang, Ronald P. Mason. Characterization of the high-resolution ESR spectra of superoxide radical adducts of 5-(diethoxyphosphoryl)-5-methyl-1-pyrroline N-oxide (DEPMPO) and 5,5-dimethyl-1-pyrroline N-oxide (DMPO). Analysis of conformational exchange, *Free Radic Res.* **2005**, *39*(8):825–36. "Characterization of the high-resolution ESR spectra of superoxide radical adducts of 5-(diethoxyphosphoryl)-5-methyl-1-pyrroline N-oxide (DEPMPO) and 5,5-dimethyl-1-pyrroline N-oxide (DMPO). Analysis of conformational exchange".
20. Roubaud, V.; Lauricella, R.; Bouteiller, J. C.; Tuccio, B. *Arch. Biochem. Biophys.* **2002**, *397*, 51.
21. Stolze, K.; Rohr-Udilova, N.; Hofinger, A.; Rosenau, T. *Bioorg. Med. Chem.* **2008**, *16*, 8082.
22. Dikalov, S. I.; Mason, R. P. *Free Radical Biol.Med.* **2001**, *30*, 187.
23. Culcasi, H.; Rockenbauer, A.; Mercier, A.; Clément, J.-L.; Pietri, S. *Free Radical Biol. Med.* **2006**, *40*, 1524.